

Ferromagnetism and exchange bias in a diluted magnetic ferroelectric oxide

L. B. Luo,¹ Y. G. Zhao,^{1,*} H. F. Tian,¹ J. J. Yang,¹ J. Q. Li,² J. J. Ding,³ B. He,³ S. Q. Wei,³ and C. Gao³

¹*Department of Physics and State Key Laboratory of New Ceramics and Fine Processing, Tsinghua University, Beijing 100084, China*

²*Beijing National Laboratory for Condensed Matter Physics, Institute of Physics, Chinese Academy of Sciences, Beijing 100080, China*

³*National Synchrotron Radiation Laboratory, University of Science and Technology of China, Hefei 230029, China*

(Received 27 October 2008; revised manuscript received 6 January 2009; published 23 March 2009)

We report on the observations of room-temperature ferromagnetism and ferroelectricity in the epitaxial thin film of $\text{BaTi}_{0.98}\text{Co}_{0.02}\text{O}_3$ (CBTO) with detailed structural and magnetic analyses. The films are single phase with an inhomogeneous distribution of Co^{2+} dopants in the structure. Room-temperature ferromagnetic hysteresis and ferroelectric loop were observed. Remarkably, the hysteresis loops for field cooling show the exchange bias and training effects. The complex magnetic behavior of CBTO was interpreted in the frame of bound magnetic polaron formation with inhomogeneity of dopant distribution. This work also demonstrated that exchange bias can be a helpful technique in exploring the mechanism of dopant-induced ferromagnetism.

DOI: 10.1103/PhysRevB.79.115210

PACS number(s): 75.50.Pp, 75.70.Ak

I. INTRODUCTION

Currently, ferromagnetism in diluted magnetic oxides (DMOs) is one of the most interesting new problems in magnetism and it is also a challenge to our understandings of the origin of magnetism. Besides the importance for fundamental issues in magnetism, DMOs with ferromagnetic ordering at room temperature are also favorable for applications in spintronics.^{1,2} Up to now, the magnetism in DMOs has not been well understood although great effort has been made. It was proposed that the ferromagnetism may originate from the impurity cluster formation in certain growth conditions;³ however, the observed magnetic signal cannot be simply explained as the extrinsic effect⁴⁻⁶ and the interpretation of these experimental phenomena remains as an open issue. Among these DMOs, the ferromagnetism observed in insulating oxides is especially interesting⁷⁻⁹ since the carrier-mediated exchange mechanism, widely accepted in (III, Mn)V semiconductors, does not apply here.¹⁰ Recently, Coey *et al.*¹¹ proposed that magnetic exchange in the insulating DMOs can be mediated by the bound magnetic polarons (BMPs),¹² and the magnetic phase diagram includes ferromagnetism (FM), antiferromagnetism (AFM), spin glass (SG), etc., depending on the cation and donor polaron concentration. While calculations were based on random distributions of dopant ions, some experiments on DMOs (Refs. 7 and 13) and other semiconductors¹⁴ indicated a remarkable fluctuation of the dopant concentration in the nanometer scale. In this case, there will be regions with different magnetic properties, and the coupling between these regions within the DMO is conceivable. However, magnetic behavior supporting this scenario has not been reported yet.

In this paper, we examine the case of cobalt doping in a highly insulating and ferroelectric oxide of BaTiO_3 . The selection of BaTiO_3 (BTO) is guided by its well-known ferroelectric properties. The Co dopants have been used in several magnetic-doped ferroelectric oxides, indicating the existence of ferromagnetism in this system.⁹ We performed detailed investigations on the structure and magnetic properties of epitaxial thin films of Co-doped BaTiO_3 (CBTO) and found

that this system shows a complex magnetic behavior, which is consistent with the BMP model with microscopic dopant nonuniformity.

II. EXPERIMENT

The CBTO films were grown on (001)-oriented SrTiO_3 (STO) substrates by pulsed laser deposition from a target with a nominal composition of $\text{BaTi}_{0.98}\text{Co}_{0.02}\text{O}_3$. The deposition temperature was 770 °C and the oxygen partial pressure was 0.1 Pa for deposition and 0.8 atm for cooling down. A Rigaku diffractometer and a Tecnai-F20 (200 kV) transmission electron microscope (TEM) with energy dispersive spectroscopy (EDS) were used in the structure analysis. X-ray-absorption near-edge spectrum (XANES) at the Co *K* edge was measured at the U7C (XAFS) end station of NSRL to determine the oxidation state of the Co dopants in the BaTiO_3 lattice. The magnetic measurements were carried out using a Quantum Design MPMS XL7. Ferroelectric polarization was investigated using a Radiant Premier II, with an Au/CBTO/ $\text{YBa}_2\text{Cu}_3\text{O}_7$ /STO structure.

III. RESULTS AND DISCUSSION

Figure 1(a) shows x-ray-diffraction patterns of the CBTO thin film, indicating single-phase characteristics with *c* axis normal to the STO surface. The TEM observation was carried out on a well-characterized sample, and the result shows a clear interface and epitaxial growth of the film [Figs. 1(b) and 1(c)]. The high quality of the film is obvious from the high-resolution TEM observation [Fig. 1(c)]. There are some structural defects in the regions near the interface [Fig. 1(b)], owing to the lattice mismatch between the film and the substrate (indicated by spot splitting in the high-index electron diffraction). We have performed FFTs for the film on local areas. The insets of Fig. 1(b) show the FFT patterns of area with visible structural defects and invisible defects, and the results are quite similar. Our careful examinations in both the CBTO film and the interfacial region indicate the high qual-

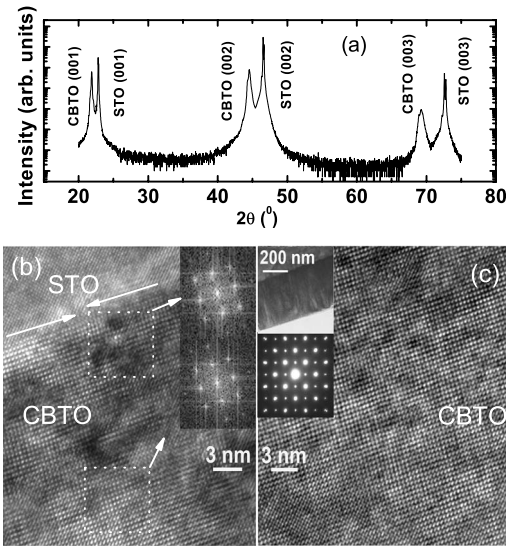


FIG. 1. (a) X-ray-diffraction (XRD) pattern of the CBTO film on STO. (b) High-resolution TEM image of the cross-sectional specimen of CBTO film in the [001] zone. The insets show the fast Fourier transform (FFT) images of typical areas with visible defects and that without visible defects, respectively. (c) High-resolution TEM image of the CBTO films far from the interface. The insets are the selected area diffraction pattern and the low magnification image of the interface of the sample.

ity of our sample and demonstrate that Co nanoclusters do not exist in it.

To find out the fine structure of the Co dopants, we performed the XANES measurement to characterize their valence and spatially resolved EDS to probe their distributions. Figure 2(a) shows Co *K*-edge absorption of the CBTO thin film, in which the onset and the shape are quite different from that of Co metal. In contrast, the onset of the absorption spectra of CBTO has a close match to that of CoO with an oxidation state of +2. So the Co dopants are expected to be in the +2 state in CBTO. It is noted that the spectra of CoO shows an absorption peak at 34 eV, which is absent in the spectra of CBTO. This is possibly due to a distorted octahedral coordination of Co atoms in the BTO lattice as proposed for Co-doped TiO_2 .⁷ During the EDS measurements, line scans of the Co distributions (with resolution of about 3–4 nm) in the interface regions and within the film were performed. Typical scanning TEM (STEM) image and line scan of Co $K\alpha$ intensity distributions are presented in Fig. 2(b) and the right panel. Line scan along lines A and B exhibits a sharp increase across the interface, confirming the existence of Co ions in the film, while the Co intensity distributions in the film along the directions both perpendicular (line C) and parallel to the interface (line D) show remarkable fluctuations, revealing a nonuniform distribution of Co ions. Furthermore, there are no evidences of Co congregations in the interface, near the film surface. Similar dopant inhomogeneity was also reported in Co-doped TiO_2 ,⁷ and it is even more prominent in the thin films grown on high-quality substrates,¹³ suggesting it as an intrinsic property. For Cr-doped ZnTe,¹⁴ spinodal decomposition-induced regions with low and high concentrations of the magnetic dopants were

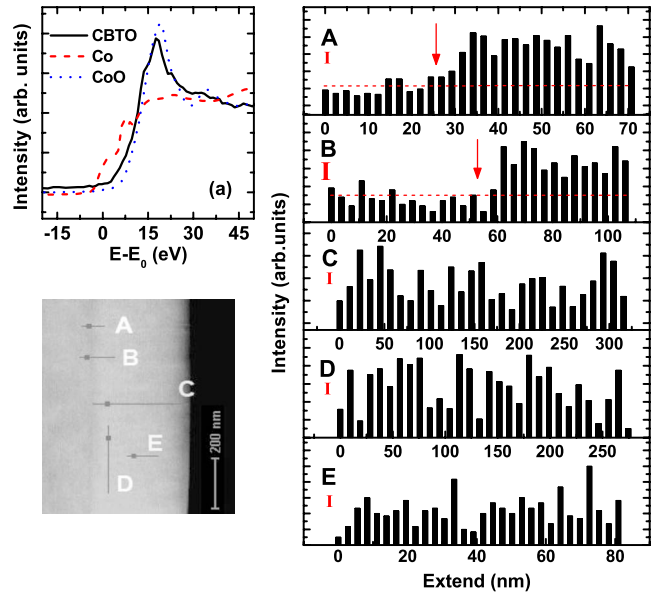


FIG. 2. (Color online) (a) Co *K*-edge XANES spectra for CBTO film with reference samples of Co metal and CoO. (b) Scanning TEM image of the CBTO film on STO and typical line scan image across the interface (A,B), (c) perpendicular to the interface, and (d) parallel to the interface, indicating the Co distributions. The dashed lines of A and B indicate the estimated background signals and the arrows indicate the interface. The error bars are shown below the labels.

also observed in the EDS experiments¹⁴ and were explained by the chemical pair interaction between dopant ions.¹⁵

The CBTO thin films are highly insulating with a resistivity of about $10^{13} \Omega \text{ cm}$ at 300 K. Quasistatic ferroelectric measurements with various frequencies [Fig. 3(a)] at 300 K indicate a well-defined ferroelectric hysteresis of the film, demonstrating room-temperature ferroelectricity. The magnetizations of the CBTO film [Fig. 3(b)] also show a remarkable hysteresis, suggesting ferromagnetism in it. The saturation moment per Co ion is $0.39\mu_B$ and the coercivity (H_c) is 153 Oe at 300 K. For comparison, the undoped BTO film was also grown under the same conditions and it exhibits only diamagnetism (not shown here) without hysteresis. In addition, the CBTO films show a significant remnant magnetization (RM), while the BTO film only exhibits a constant background signal [Fig. 3(c)]. Figure 3(d) shows the magnetization as a function of temperature under zero-field cooled (ZFC) and field cooled (FC). The ZFC and FC curves exhibit divergences at low temperatures, and the splitting is smaller under larger fields. This result will be discussed later.

In order to investigate possible magnetic coupling within the film, we measured the *M-H* curves of the film after ZFC and FC processes [Fig. 4(a)]. The FC loop at 10 K exhibits a negative shift with respect to the cooling field, while the ZFC loop lies symmetrically about the origin. Such a negative shift is the hallmark of exchange bias (EB), which was observed in systems containing FM-AFM or FM-SG interface.¹⁶ In addition, the magnitude of the shift decreases when the loop measurements were repeated, consistent with the well-known training effect in the EB system.¹⁶ To increase the precision, the FC loops measurements were per-

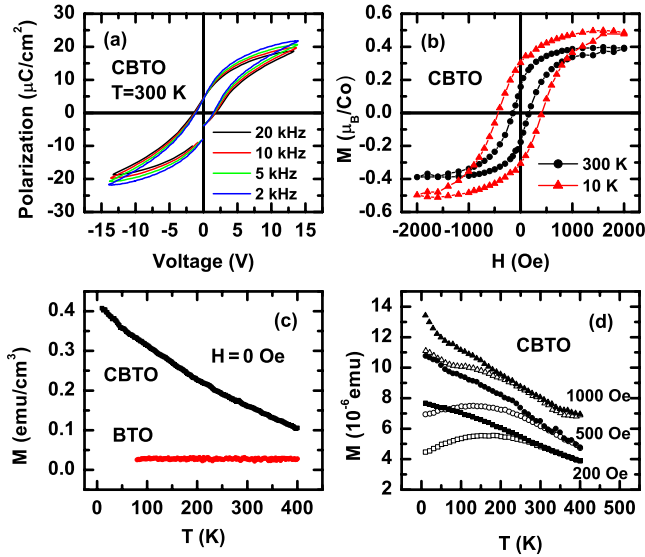


FIG. 3. (Color online) (a) Ferroelectric hysteresis loops of CBTO thin film at 300 K. (b) Magnetic hysteresis loops of the CBTO thin film at 300 and 10 K. (c) Remnant magnetizations as a function of temperature of CBTO film and the undoped BTO film. (d) ZFC (open symbols) and FC (solid symbols) M - T curves measured at different fields.

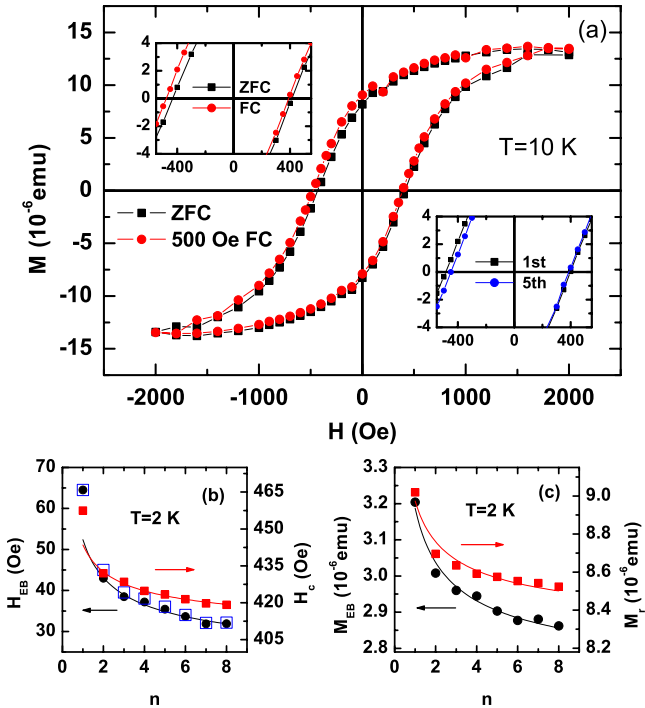


FIG. 4. (Color online) Top panel: (a) hysteresis loops of the CBTO film at 10 K after ZFC and FC processes. The upper inset and the lower inset display the enlarged view of loops after ZFC and FC process, the first, and the fifth field cycles after FC process. Bottom panel: (b) H_{EB} and H_c and (c) M_{EB} and M_r as functions of the field cycle number after field cooling (500 Oe) measured at 2 K. The open symbols show the data obtained from the recursive formula.

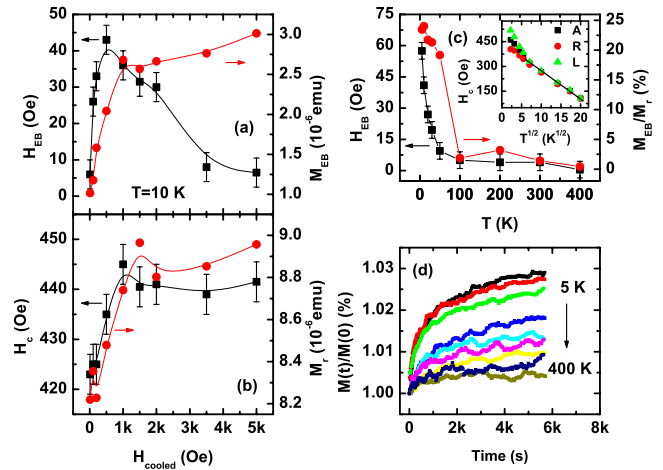


FIG. 5. (Color online) Cooling-field dependence of (a) H_{EB} and H_c and (b) M_{EB} and M_r of CBTO film at 10 K. (c) Temperature dependence of H_{EB} and normalized M_{EB} of CBTO film after FC at 500 Oe. The inset shows the coercive field as a function of temperature (H_c vs $T^{1/2}$). (d) Magnetization relaxations are measured at 5, 10, 20, 30, 50, 100, 200, 300, and 400 K with the magnetic field of $1.3H_c(T)$ after ZFC processes.

formed at 2 K, where H_{EB} , defined as the transverse shift of the gravity center of the loop, is much larger. The cycle (n) dependence of H_{EB} of the film at 2 K follows a simple power law for $n > 1$: $H_{EB} - H_{EB\infty} = H_0 / \sqrt{n}$ (Ref. 17) with $H_{EB\infty} = 20.6$ Oe and $H_0 = 31.8$ Oe. According to the nonequilibrium thermodynamics theory,¹⁸ the training effect is caused by the spin configurational relaxation in the FM-AFM interface. The $H_{EB}(n)$ in the CBTO film is described by a recursive formula $H_{EB}(n+1) - H_{EB}(n) = -\gamma [H_{EB}(n) - H_{EB\infty}]^3$,¹⁸ where the sample-dependent constant $\gamma = 1.8 \times 10^{-4}$ Oe⁻². Moreover, the EB magnetization for $n > 1$ (M_{EB} , defined as the vertical shift of the RM), the average measure of the RM (M_r), and the coercivity (H_c) all can be fitted by the simple power-law formula.

To further characterize the magnetic coupling within the film, the cooling-field (H_{cooled}) dependence of the EB effect of the CBTO film at 10 K was investigated. Figure 5(a) shows that H_{EB} increases with increasing H_{cooled} when H_{cooled} is small, then reaches a maximum at about $H_{cooled} = 500$ Oe, and finally reduces to zero at $H_{cooled} = 5000$ Oe. Similar behavior of H_{EB} has also been reported in perovskite cobaltite $La_{1-x}Sr_xCoO_3$ with phase separation, and it was interpreted in terms of spin disorder in the interfaces and the growth of the FM clusters.¹⁹ In the CBTO film, the increasing cooling field always enhances the alignment degree of the moment of FM regions.^{19,20} When H_{cooled} is small, the spin disorder at the interface is reduced with increasing H_{cooled} as shown by the increase in M_{EB} , H_c , and M_r , leading to the enhancement of FM-AFM or FM-SG coupling and the resultant increase in H_{EB} . When H_{cooled} is larger than 500 Oe, the sizes of the FM regions are also increased, leading to larger FM-AFM (or FM/SG) proportion. In this case, it is more difficult for the spins of AFM or SG region around to bias that of FM regions. It should be pointed out that the exchange bias field is usually smaller when FM layer is thicker in FM-AFM systems.^{16,19}

Figure 5(c) display the temperature variations of the H_E and M_E , measured at the cooling field of 500 Oe. It clearly shows that the EB effect disappears at about 100 K. The inset of Fig. 5(c) shows that the coercive field exhibits as $H_c \propto T^{1/2}$ above 100 K, indicating a single-domain behavior.²¹ A transition temperature of 700 K is estimated from the extrapolation of H_c - T relation. The ZFC magnetization relaxation was measured at different temperatures, with a fixed measuring field of $1.3H_c(T)$. The magnetization below 100 K does not display any sign of saturation even after 5000 s, indicating that the system is far from the equilibrium. In contrast, the magnetization above 100 K only shows fluctuations after 2000 s. Such a long-time magnetization relaxation was also observed in the glassy compound when the field is larger than the coercive field.²²

To understand the magnetism in the CBTO film, one of the crucial questions is where the FM signals come from. It can be concluded from the $H_c \propto T^{1/2}$ relation that the FM regions are single domains, and what is the nature of these FM regions? If the FM regions are Co metal nanoclusters, the coercivity for the noninteracting single-domain particles with a uniaxial anisotropy follows $H_c = H_{c,0}(1 - \sqrt{\frac{25k_B T}{KV}})$, where K is the anisotropy energy density and V is the particle volume.²¹ Using $K = 4.5 \times 10^6$ erg/cm³ for Co metal,^{3,21} and the H_c - T curve, the diameter of the particles was estimated to be 10 nm. However, as mentioned previously, the XANES results show that Co dopants in CTBO films are in the +2 state, and the careful TEM investigation also rules out the possibility of Co metal nanocluster formation.

As the EB effect is frequently observed in the systems with FM-AFM interface, another possibility that should be considered is the formation of CoO (well known as an AFM compound) nanocluster in the present film. When the size of the CoO cluster is reduced to several nanometers, uncompensated spins on the surface may reach an appreciable net magnetic moment at low temperatures. The strong coupling between the uncompensated spins and the CoO nanocluster is expected to result in large H_c and H_{EB} .²³ For example, Gruyters²⁴ showed that granular CoO films display hysteresis loops below 250 K and H_c and H_{EB} are 3.35 kOe and 5.15 kOe at 10 K, respectively. In contrast, the CBTO films exhibit ferromagnetic hysteresis at and above room temperature, and both H_c (440 Oe at 10 K) and H_{EB} (41 Oe at 10 K) are much smaller than that reported by Gruyters,²⁴ indicating that the observed magnetic signals are not likely to originate from CoO nanocluster. It is noted that there are also some reports about monodispersed CoO nanoparticles, but such nanoparticles are not expected to form in thin films.

The above analysis indicates that Co or CoO nanocluster cannot account for the magnetism of CBTO films, and the BMP model proposed by Coey *et al.*¹¹ seems applicable here. In CTBO thin film, the Co distribution mapping confirmed that Co ions decomposed into dopant-rich and dopant-poor regions. The oxygen vacancies in the film tend to appear in the proximity of Co ions to keep charge neutrality, leading to the formation of BMP. With a proper polaron concentration, the neighboring BMPs are likely to overlap and interact to

create ferromagnetism. Meanwhile, other regions with different concentrations of Co ions may be AFM or SG. The EB effect can be interpreted as the consequence of the interaction of FM regions with the AFM (or SG) regions. Considering the EDS scan results and the coercivity behavior of CBTO, we estimated that the size of FM regions is from several nanometers to a few dozen nanometers. Finally, we tried to analyze the dopant inhomogeneity from the transition temperature. In the BMP model,¹¹ the transition temperature is described by

$$T_c = [(S+1)s^2x\delta/3]^{1/2} J_{sd} f_o (r_c^{\text{eff}}/r_o)^3 / k_B,$$

where S and s are the spin of the Co²⁺ dopant and the donor electron, respectively, x is the doping concentration, δ is the donor concentration, J_{sd} is the s - d exchange parameter, f_o is the oxygen packing fraction of BaTiO₃, r_c^{eff} is the effective cation radius, r_o is the oxygen radius, and k_B is the Boltzmann constant. Using $T_c = 700$ K, $f_o = 0.54$ (calculated), $J_{sd} = 3.15$ eV (Ref. 25) for CBTO, and $S = 3/2$, $s = 1/2$, $\delta = 0.01$, $r_c^{\text{eff}} = 0.20$ nm, and $r_o = 0.14$ nm in typical cases,^{9,11} the doping concentration is estimated to be $x = 7.1\%$, which is larger than the nominal value of 2%. This is consistent with the interpretation that the ferromagnetism originates from the regions with higher Co dopant concentrations. It is noted that in the case of Mn-doped InAs, the extended x-ray-absorption fine-structure technique also indicated that Mn impurity ions are not randomly distributed but form their local structure.²⁶ This short-range order²⁶ and the local fluctuation in dopant density²⁷ are expected to enhance the Curie temperature in Mn-doped InAs and other similar system.

It can also be concluded that the single-phase CBTO films are simultaneously ferroelectric and ferromagnetic at room temperature, manifesting itself as a multiferroic material.^{28,29} Multiferroic materials that exhibit simultaneous ferroelectric and ferromagnetic orderings are of great interest for potential applications, but those are very limited in single-phase compounds.³⁰ Since the oxygen vacancies play a central role in the ferromagnetism, the modulation of magnetism by electric field as demonstrated in Co-doped TiO₂ (Ref. 31) is conceivable. Further study of the possible magnetoelectric coupling in CBTO film is deserved.

In summary, room-temperature ferromagnetism and ferroelectricity were observed in CBTO. CBTO also shows complex magnetic behaviors including the EB and training effects, as well as the glassy behavior, which was interpreted in the BMP model with the inhomogeneity of dopant distribution. This work could be helpful for shedding light on the mechanism of dopant-induced ferromagnetism in insulators and exploring multiferroics via doping of ferroelectric compounds.

ACKNOWLEDGMENTS

This work was supported by the National Science Foundation of China (Grants No. 50872065 and No. 50425205) and National 973 Project (Grant No. 2009CB929202).

*ygzha@tsinghua.edu.cn

- ¹W. Prellier, A. Fouchet, and B. Mercey, *J. Phys.: Condens. Matter* **15**, R1583 (2003); R. Janisch, P. Gopal, and N. A. Spaldin, *ibid.* **17**, R657 (2005); T. Fukumura, H. Toyosaki, and Y. Yamada, *Semicond. Sci. Technol.* **20**, S103 (2005).
- ²Y. Matsumoto, M. Murakami, T. Shono, T. Hasegawa, T. Fukumura, M. Kawasaki, P. Ahmet, T. Chikyow, S. Koshihara, and H. Koinuma, *Science* **291**, 854 (2001); K. Ueda, H. Tabata, and T. Kawai, *Appl. Phys. Lett.* **79**, 988 (2001).
- ³S. R. Shinde, S. B. Ogale, J. S. Higgins, H. Zheng, A. J. Millis, V. N. Kulkarni, R. Ramesh, R. L. Greene, and T. Venkatesan, *Phys. Rev. Lett.* **92**, 166601 (2004).
- ⁴H. Toyosaki, T. Fukumura, Y. Yamada, and M. Kawasaki, *Appl. Phys. Lett.* **86**, 182503 (2005); K. Mamiya, T. Koide, A. Fujimori, H. Tokano, H. Manaka, A. Tanaka, H. Toyosaki, T. Fukumura, and M. Kawasaki, *ibid.* **89**, 062506 (2006).
- ⁵J. R. Neal, A. J. Behan, R. M. Ibrahim, H. J. Blythe, M. Ziese, A. M. Fox, and G. A. Gehring, *Phys. Rev. Lett.* **96**, 197208 (2006).
- ⁶Y. G. Zhao, S. R. Shinde, S. B. Ogale, J. Higgins, S. E. Lofland, C. Lanci, J. P. Buban, N. D. Browning, S. Das Sarma, A. J. Millis, V. N. Kulkarni, R. J. Choudhary, R. L. Greene, and T. Venkatesan, *Appl. Phys. Lett.* **83**, 2199 (2003); G. Herranz, R. Ranchal, M. Bibes, H. Jaffrès, E. Jacquet, J.-L. Maurice, K. Bouzehouane, F. Wyczisk, E. Tafra, M. Basletic, A. Hamzic, C. Colliex, J.-P. Contour, A. Barthélémy, and A. Fert, *Phys. Rev. Lett.* **96**, 027207 (2006).
- ⁷K. A. Griffin, A. B. Pakhomov, C. M. Wang, S. M. Heald, and Kannan M. Krishnan, *Phys. Rev. Lett.* **94**, 157204 (2005).
- ⁸A. J. Behan, A. Mokhtari, H. J. Blythe, D. Score, X.-H. Xu, J. R. Neal, A. M. Fox, and G. A. Gehring, *Phys. Rev. Lett.* **100**, 047206 (2008).
- ⁹C. Song, F. Zeng, Y. X. Shen, K. W. Geng, Y. N. Xie, Z. Y. Wu, and F. Pan, *Phys. Rev. B* **73**, 172412 (2006); Y. H. Lin, S. Y. Zhang, C. Y. Deng, Y. Zhang, X. H. Wang, and C. W. Nan, *Appl. Phys. Lett.* **92**, 112501 (2008); L. B. Luo, Y. G. Zhao, H. F. Tian, J. J. Yang, H. Y. Zhang, J. Q. Li, J. J. Ding, B. He, S. Q. Wei, and C. Gao, *ibid.* **92**, 232507 (2008).
- ¹⁰T. Dietl, *Semicond. Sci. Technol.* **17**, 377 (2002); T. Jungwirth, J. Sinova, J. Mašek, J. Kučera, and A. H. MacDonald, *Rev. Mod. Phys.* **78**, 809 (2006).
- ¹¹J. M. D. Coey, M. Venkatesan, and C. B. Fitzgerald, *Nature Mater.* **4**, 173 (2005).
- ¹²A. C. Durst, R. N. Bhatt, and P. A. Wolff, *Phys. Rev. B* **65**, 235205 (2002); A. Kaminski and S. Das Sarma, *Phys. Rev. Lett.* **88**, 247202 (2002).
- ¹³K. A. Griffin, M. Varela, S. J. Pennycook, A. B. Pakhomov, and K. M. Krishnan, *J. Appl. Phys.* **99**, 08M114 (2006).
- ¹⁴S. Kuroda, N. Nishizawa, K. Takita, M. Mitome, Y. Bando, K. Osuch, and T. Dietl, *Nature Mater.* **6**, 440 (2007).
- ¹⁵T. Fukushima, K. Sato, H. Katayama-Yoshida, and P. H. Dederichs, *Phys. Status Solidi A* **203**, 2751 (2006).
- ¹⁶J. Nogués and I. K. Schuller, *J. Magn. Magn. Mater.* **192**, 203 (1999).
- ¹⁷D. Paccard, C. Schlenker, O. Massenet, R. Montmory, and A. Yelon, *Phys. Status Solidi* **16**, 301 (1966).
- ¹⁸C. Binek, *Phys. Rev. B* **70**, 014421 (2004).
- ¹⁹Y. K. Tang, Y. Sun, and Z. H. Cheng, *Phys. Rev. B* **73**, 174419 (2006); Y.-k. Tang, Y. Sun, and Z.-h. Cheng, *J. Appl. Phys.* **100**, 023914 (2006).
- ²⁰D. Niebieskikwiat and M. B. Salamon, *Phys. Rev. B* **72**, 174422 (2005).
- ²¹B. D. Cullity, *Introduction to Magnetic Materials* (Addison-Wesley, Reading, MA, 1972).
- ²²K. Binder and A. P. Young, *Rev. Mod. Phys.* **58**, 801 (1986); E. Vincent, J. Hammann, M. Ocio, J. P. Bouchaud, and L. F. Cugliandolo, in *Proceedings of the XIVth Sitges Conference, Barcelona, 1996*, Lecture Notes in Physics Vol. 492 (Springer, Berlin, New York, 1997), p. 184.
- ²³T. Ambrose and C. L. Chien, *Phys. Rev. Lett.* **76**, 1743 (1996).
- ²⁴M. Gruyters, *EPL* **77**, 57006 (2007).
- ²⁵R. C. Casella and S. P. Keller, *Phys. Rev.* **116**, 1469 (1959).
- ²⁶Y. L. Soo, S. Kim, Y. H. Kao, A. J. Blattner, S. Wessels, S. Khalid, C. Sanchez Hanke, and C.-C. Kao, *Appl. Phys. Lett.* **84**, 481 (2004).
- ²⁷G. Bouzerar, T. Ziman, and J. Kudrnovsky, *Appl. Phys. Lett.* **85**, 4941 (2004); B. W. Wessels, *New J. Phys.* **10**, 055008 (2008).
- ²⁸W. Eerenstein, N. D. Mathur, and J. F. Scott, *Nature (London)* **442**, 759 (2006); S.-W. Cheong and M. Mostovoy, *Nature Mater.* **6**, 13 (2007).
- ²⁹D. I. Khomskii, *J. Magn. Magn. Mater.* **306**, 1 (2006).
- ³⁰N. A. Hill, *J. Phys. Chem. B* **104**, 6694 (2000).
- ³¹T. Zhao, S. R. Shinde, S. B. Ogale, H. Zheng, T. Venkatesan, R. Ramesh, and S. Das Sarma, *Phys. Rev. Lett.* **94**, 126601 (2005).